

Splitting of the subgap resistance peak in superconductor/two-dimensional electron gas contacts at high magnetic fields

D. Uhlisch, S. G. Lachenmann, Th. Schäpers, A. I. Braginski, and H. Lüth
Institut für Schicht- und Ionentechnik, Forschungszentrum Jülich, D-52425 Jülich, Germany

J. Appenzeller
II. Physikalisches Institut, RWTH-Aachen, D-52056 Aachen, Germany

A. A. Golubov
Faculty of Applied Physics, University of Twente, 7500 AE Enschede, The Netherlands

A. V. Ustinov
Physikalisches Institut III, Universität Erlangen-Nürnberg, Erwin-Rommel Straße 1, 91508 Erlangen, Germany
 (Received 27 October 1999)

The differential resistance of NbN/two-dimensional electron gas (2DEG) contact is measured at high magnetic fields. In zero magnetic field the contact shows a pronounced resistance peak at zero bias due to a high barrier at the NbN/2DEG interface, which decreases if a magnetic field is applied in the plane of the 2DEG. For a magnetic field oriented perpendicular to the plane of the 2DEG, not only the zero-bias resistance decreases but so does the normal-state resistance which drops to vanishingly small values. A pronounced substructure due to a splitting of the resistance peak into a three-peak structure is observed at high perpendicular fields. We suggest that the appearance of this substructure can be explained by multiple Andreev reflections due to skipping orbits of electrons and holes accompanied by inelastic scattering in the 2DEG near the interface.

In the past, most investigations concerning the magnetotransport in normal-metal (N) / superconductor (S) structures have been focused on the regime of low magnetic fields, where phase coherent mechanisms are of importance.¹⁻³ The magnetic-field induced phase differences manifest themselves in oscillating sample resistances due to interference phenomena. For a quantum point contact next to a SN interface Takayanagi⁴ could show that zero bias conductance maximum is suppressed by a magnetic field. This effect is explained in terms of Andreev reflection and ballistic transport in the normal region.

In all those studies, the superconductor is in the Meissner phase and the influence of the magnetic field on the transport in the normal region is small. Only very recently experiments with samples consisting of a two-dimensional electron gas (2DEG) and NbN or AuSn electrodes have been reported. Measurements have been performed at very high magnetic fields^{5,6} and edge state transport was investigated in the quantum Hall regime.

Here, we present measurements performed with single NbN/2DEG contacts in high magnetic fields. For a magnetic field in the plane of the 2DEG we observed a decrease of the zero-bias resistance peak with increasing magnetic field. In contrast to that, we find that this resistance peak splits into a three-peak structure when a magnetic field larger than approximately 250 mT is applied perpendicular to the plane of the 2DEG. We propose a simple model which shows that the interplay between energy-dependent Andreev reflection and inelastic scattering in the 2DEG can be responsible for the observed feature.

Our experiments have been performed with a GaInAs/InP heterostructure grown by metal organic vapor phase

epitaxy.^{7,8} The layer sequence consists of a 400-nm-thick InP buffer, a 10-nm-thick *n*-doped InP layer (doping concentration: $4.2 \times 10^{17} \text{ cm}^{-3}$), a 20-nm-thick InP spacer, a 10-nm-thick Ga_{0.23}In_{0.77}As active layer and a 150-nm-thick Ga_{0.47}In_{0.53}As cap. Since the 2DEG is located in the highly strained layer with an In content of 77%, it yields a high mobility due to a low effective electron mass of $m^* = 0.036 m_e$ and a reduced contribution of alloy scattering. Carrier concentration and mobility, measured at 4.2 K by the Hall effect and Shubnikov-de Haas effect, were found to be $n = 6 \times 10^{15} \text{ m}^{-2}$ and $\mu = 26.6 \text{ m}^2/\text{V s}$, respectively. This corresponds to a Fermi energy $E_F = 40 \text{ meV}$ and a transport mean free path of $L_{tr} = 3.4 \text{ }\mu\text{m}$.

The critical temperature of NbN which was used for the superconducting contacts was determined from resistance measurements to be $T_c = 13.6 \text{ K}$. From this T_c a superconducting gap of $\Delta_0 = 2.5 \text{ meV}$ can be calculated using Bardeen-Cooper-Schrieffer (BCS) theory under the assumption of strong coupling.^{9,10} Measurements show that at low temperatures ($T \leq 1.4 \text{ K}$) the second critical field of our 100-nm-thick NbN films exceeds 14 T for in-plane as well as for magnetic fields perpendicular to the NbN films.

The semiconductor heterostructure containing the buried 2DEG is structured into a Hall bar geometry by means of optical lithography and reactive ion etching. NbN/2DEG contacts is prepared by sputtering NbN directly onto the edge of the Hall bar. Prior to the deposition the 15- μm -wide 2DEG contact area is cleaned in situ by Ar plasma. Additionally, the Hall bar possesses alloyed ohmic contacts made of normal metal which are used for current injection and voltage measurement. A schematic top view of the structure is shown in Fig. 1.

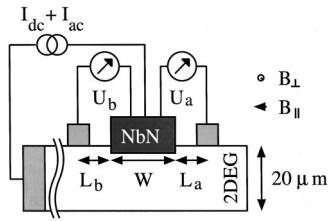


FIG. 1. Schematic of the sample layout (top view).

Using the configuration shown in Fig. 1, the differential resistance $R_c = U_a/I_{ac}$ was measured with standard lock-in technique. The injected current $I = I_{dc} + I_{ac}$ consisted of a dc current I_{dc} superimposed by a small ac current I_{ac} of 10 nA. The frequency of the ac current was 19 Hz. In this way a finite dc voltage drop U_{dc} was established at the 2DEG/NbN contact. The measurements were performed at $T = 50$ mK.

Figure 2 shows the differential resistance of a 2DEG/NbN contact as a function of the voltage drop at the interface for various magnetic fields. The magnetic field $B_{||}$ is oriented in parallel to the 2DEG along the NbN/2DEG interface, see Fig. 1. At zero bias a pronounced resistance peak is observed indicating a strong barrier at the NbN/2DEG interface. From the drop of the resistance with increasing voltages the barrier strength at the interface can be estimated. Following the Blonder-Tinkham-Klapwijk (BTK) model a barrier strength of $Z=2$ is calculated.¹¹ The shallow resistance minima are located at about ± 1.5 mV. The fact that the minima do not coincide with the calculated energy gap of 2.5 meV indicates that the density of states in NbN near the interface is not BCS-like as assumed in the BTK model. Moreover, the measured differential resistance resembles much more the one obtained for Nb/2DEG contacts discussed by Neurohr *et al.*¹² As shown in Fig. 2, applying a magnetic field in the plane of the 2DEG along the Nb/2DEG interface with increasing intensity from zero to 13.9 T, the normal-state resistance R_N for $eU_{dc} > \Delta$ remains approximately constant, while the zero-bias resistance drops monotonously. This can be explained by suppression of Andreev reflection due to pair breaking by Abrikosov vortices in NbN. Since our sample has a large Z value, the zero-bias resistance at $B=0$ is inversely proportional to the small subgap density of states in NbN. By in-

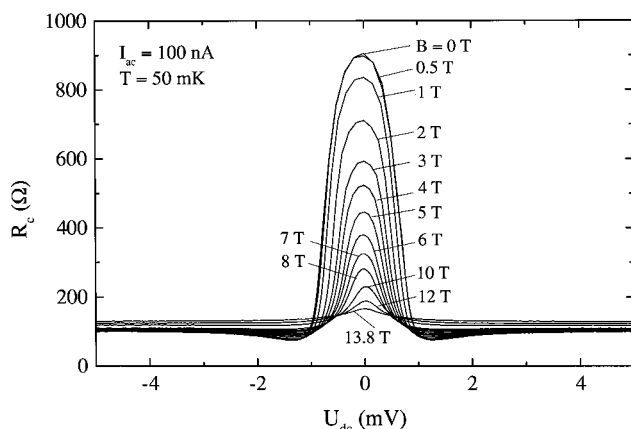


FIG. 2. Differential resistance of a NbN/2DEG contact for various magnetic fields oriented in the plane of the 2DEG along the NbN/2DEG interface.

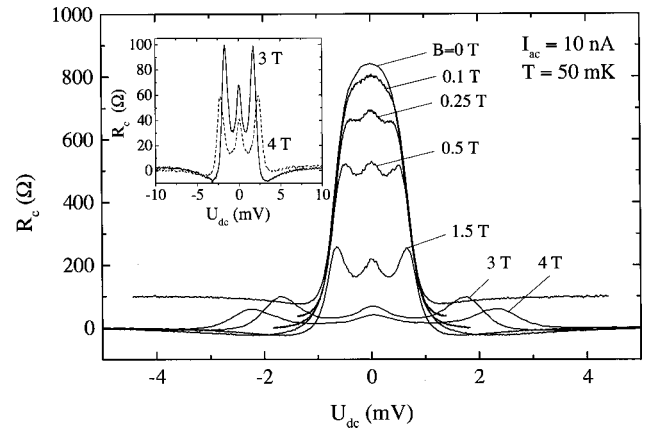


FIG. 3. Differential resistance of a NbN/2DEG contact for various magnetic fields oriented perpendicular to the 2DEG. The inset shows the sample layout and measurement configuration. In the measurement the voltage U_a is detected. $W = 15$ μm ; $L_a = L_b = 5$ μm . The inset shows the curves for $B = 3$ T and 4 T in more detail.

creasing the magnetic field subgap states are created by the pair breaking effect.^{13,14} This increased density of states thus leads to a decrease of the zero-bias resistance.

In Fig. 3 the different resistance $R_c = U_a/I_{ac}$ is plotted as a function of the voltage drop at the interface for a magnetic field B_{\perp} oriented perpendicular to the 2DEG. Here, R_c is determined from the voltage U_a , where for a magnetic-field vector pointing out of the sample surface no Hall voltage contribution is present. In contrast, when calculating the energy eU_{dc} of the electrons in the 2DEG with respect to the superconducting contact, the Hall voltage $U_H = B_{\perp} I_{ac}/(ne)$ has to be taken into account.¹⁵ The Hall voltage is included if the voltage U_b between the NbN electrode and the other contact next to the NbN electrode is measured. Neglecting the longitudinal resistance of the 2DEG (Ref. 16) this voltage is $U_b = U_a + U_H$ for a magnetic field pointing out of the 2DEG plane. The total voltage drop at the 2DEG-NbN interface U_{dc} in Fig. 3 was thus calculated by integrating the differential resistance $R_b = U_b/I_{ac}$ with respect to I_{dc} .

There are three features in Fig. 3 which are not observed in the measurements performed in magnetic fields in the plane of the 2DEG: (i) R_N drops to vanishingly small values for $B \geq 0.25$ T. (ii) The zero-bias resistance peak splits into three peaks. (iii) The complete structure broadens for $B \geq 3$ T.

Feature (iii) shows that the calculated voltage drop U_{dc} gives only an approximate value for the true dc voltage drop at the NbN/2DEG interface. For the applied fields which are much smaller than the second critical field of NbN one would expect a constant width of the resistance peak as it is observed for in-plane fields. The deviation most probably arises from the fact that for high enough fields the drop of the Hall voltage is no longer exactly located at the NbN/2DEG interface but partly takes place in the 2DEG itself. This might be attributed to the existence of edge states which form in the 2DEG and leads to the occurrence of a so called *hot spot* near the current contact.¹⁷ Within the region of the hot spot dissipation and thus a voltage drop takes place in the 2DEG close to the interface.

The fact that features (i) and (ii) only occur in perpendicu-

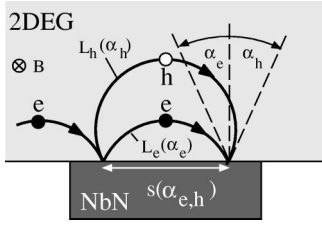


FIG. 4. Skipping orbits of an electron “e” incident from the left which is either normally reflected as an electron or Andreev reflected as a hole “h.”

lar magnetic fields leads to the conclusion that they are related to skipping orbits of electrons in the 2DEG. We already showed in a previous paper that multiple tunneling attempts due to skipping orbits lead to a strong suppression of the contact resistance.¹⁸ This mechanism can thus be used to explain the drop of R_c to zero for voltages U_{dc} above 4 mV. In the following model we suggest that also the splitting of the subgap resistance peak can be explained within this framework.

As shown in Fig. 4, ballistic electrons in the 2DEG move along the sample boundary following so-called skipping orbits, the classical analogue to edge states.¹⁹ At the S/2DEG contact they are either transmitted through the NbN/2DEG interface or reflected. The reflection process can either be a normal or an Andreev reflection process.²⁰ In the latter case the particle is converted into a particle of opposite charge, e.g., an electron into a hole. Let us assume an electron at the Fermi level incident at the 2DEG/NbN interface as shown in Fig. 4. In the normal specular reflection process an electron leaves the interface at the same angle as the incoming electron. In the Andreev reflection process the holes are retroreflected in the same direction as the incident electron. In contrast to the zero magnetic field case, the Andreev reflected hole does not trace back the path of the incident particle in a finite field. However, at the 2DEG/NbN interface the trajectory of the incident electron at the Fermi energy and the Andreev reflected hole are tangential due to the change of sign of the velocity. Due to the opposite effective mass and the inverse charge the hole path has the same curvature as the trace of the reflected electron. Increasing the magnetic field decreases the radius of the cyclotron orbit $r_c = \hbar k_F / (eB)$ (k_F : Fermi wave number) and leads to a shorter distance $s(\alpha_{e,h}) = 2r_c \cos(\alpha_{e,h})$. Here $\alpha_{e,h}$ is the reflection angle for electrons (e) and holes (h), respectively. For particle at the Fermi level, α_e and α_h have the same magnitude. The total number of collisions with the boundary and consequently the resulting effective transmission probability increases with magnetic field.¹⁸ This is the reason for the suppression of R_N observed with increasing B_\perp in the measurement shown in Fig. 3.

Based on the skipping orbit picture, we have estimated the differential resistance as a function of U_{dc} . For simplicity, the NbN/2DEG contact is approximated by the BTK model.¹¹ Transport in the 2DEG as well as across the interface is regarded to take place ballistically. Since only magnetic fields which are considerably lower than the second critical field of NbN are considered, any influence of the magnetic field on the density of states in NbN is neglected. Under these assumptions, the only process which may con-

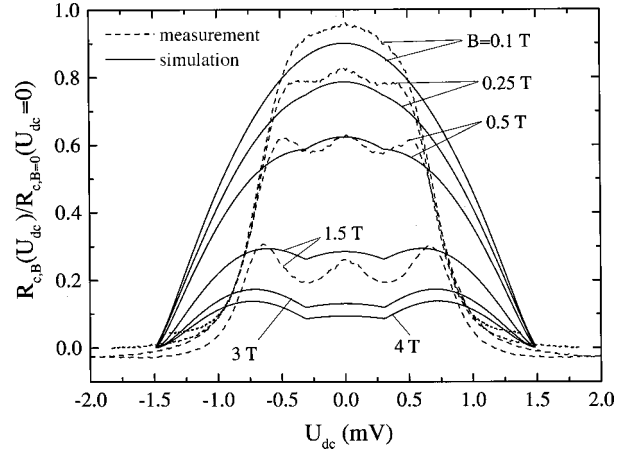


FIG. 5. Simulated normalized differential resistance for different magnetic fields (solid lines). The dashed curves represent the corresponding measured differential resistance for $B=0.1$ T, $B=0.25$ T, $B=0.5$ T, and $B=1.5$ T.

tribute to the differential conductance for voltages $eU_{dc} < \Delta$ is Andreev reflection.²⁰ For an electron injected with energy eU_{dc} , this process leads to a retroreflection of a hole with energy $-eU_{dc}$ with respect to the electrochemical potential of the superconductor. The corresponding trajectory in real space is shown in Fig. 4. The Andreev reflection probability is approximated by the BTK expression¹¹ for $eU_{dc} < \Delta$, which is slightly modified by inserting an angle dependent Z factor: $Z(\alpha) = [1/(\eta \cos \alpha) - 1]^{1/2}$. Here, $\eta \ll 1$ is the transmission coefficient for normal incidence.¹⁸ If the energy of the particles in the 2DEG is above the Fermi level, the particles are inelastically scattered by electron-electron scattering as shown by Giuliani and Quinn.²¹ In our simulation this mechanism is incorporated by assuming a loss of particles with probability $\exp[-L_{e/h}/l_{ee}(U_{dc})]$. Here, $L_{e/h}$ is the orbit length of an electron and hole, respectively, while $l_{ee}(U_{dc})$ is the electron-electron scattering length. As shown by experiments with ballistic electrons in the AlGaAs/GaAs material system, the inelastic mean free path saturates at low temperatures if the excess energy approaches small values.²² Following this observation the underlying idea for the theoretical explanation of the three-peak structure in the differential resistance is, that this saturation of the inelastic mean free path is responsible for the two local minima shown in Fig. 3. The minima are found at an excess energy of ≈ 0.3 meV, which corresponds to a maximum electron-electron scattering length of $l_{ee,max} = 120 \mu\text{m}$. Here, the scattering length was calculated for the InGaAs semiconductor system by using the theory of Giuliani and Quinn.²¹

The result of our calculation²³ together with some of the experimental curves is shown in Fig. 5 for $\Delta_{exp} = 1.5$ meV. The barrier height is estimated from the experimental data within the BTK model to be $Z(\alpha=0) \approx 2$. As it has been mentioned above, the BTK model is not quantitatively applicable due to proximity effect. Therefore, the overall form of the resistance peaks in Fig. 5 is not very well reproduced. However, the drop of the zero bias resistance with increasing magnetic field does approximately coincide with the experimental data and the observed three-peak structure for high fields is qualitatively reproduced. The latter fact can be understood as follows: For $|eU_{dc}| < 0.3$ meV, $l_{ee}(U_{dc})$ is as

sumed to be constant. Therefore, the only energy dependence in this energy range originates from $A(U_{dc})$ which slightly increases and thereby reduces $R_c(U_{dc})$. For $|U_{dc}| > 0.3$ meV, the inelastic mean free path $l_{ee}(U_{dc})$ drastically decreases. More and more electrons are scattered inelastically out of their states at eU_{dc} . Consequently the probability for Andreev reflection at eU_{dc} decreases which leads to the observed increase of $R_c(U_{dc})$. Finally, for energies larger than about 0.6 meV, $A(U_{dc})$ strongly increases and approaches one close to the gap energy Δ_{exp} . Due to this fact, no electrons remain in states with energy eU_{dc} and therefore cannot be scattered inelastically any more. The differential contact resistance drops to zero because $\langle T_B(U_{dc}) \rangle$ becomes equal to one in this case.

The calculated and measured curves in Fig. 5 show a rather good qualitative agreement. A further improvement might be possible if more precise information on the energy dependence of the inelastic mean free path is available. For our simple model we used a sharp cutoff of l_{ee} , though naturally the l_{ee} should saturate smoothly. However, a dip in the differential resistance is expected in any case. A further improvement of the model would also be possible by taking reflec-

tions above Δ_{exp} into account. Nevertheless, these refinements are not expected to alter the triple peak structure qualitatively. The the presented model based on the interplay of inelastic scattering and Andreev reflection is one possible way to describe the general behavior of the experimental curves. Of course there might be other mechanisms which have to be considered in addition in order to obtain a quantitative agreement with the measurements.

In summary, the differential resistance of NbN/2DEG contacts has been measured at low temperatures and high magnetic fields. It is shown that a magnetic field applied in plane of the 2DEG leads to a suppression of the zero bias resistance peak. For magnetic fields perpendicular to the 2DEG a strong suppression of the contact resistance above as well as below the superconducting gap voltage has been observed. Additionally, the subgap resistance peak splits into a symmetric three-peak structure in high fields. This behavior is qualitatively interpreted by a model based on Andreev reflection and inelastic scattering of ballistic electrons in the 2DEG.

We thank H. Hardtdegen for the growth of the semiconductor heterostructures.

-
- ¹H. Pothier, S. Guéron, D. Esteve, and M. H. Devoret, Phys. Rev. Lett. **73**, 2488 (1994).
- ²S. G. den Hartog, C. M. A. Kapteyn, B. J. van Wees, T. M. Klapwijk, and G. Borghs, Phys. Rev. Lett. **77**, 4954 (1996).
- ³A. F. Morpurgo, S. Holl, B. J. van Wees, T. M. Klapwijk, and G. Borghs, Phys. Rev. Lett. **78**, 2636 (1997).
- ⁴H. Takayanagi, Physica B **227**, 224 (1996).
- ⁵H. Takayanagi, and T. Akazaki, Physica B **249-251**, 462 (1998).
- ⁶T. D. Moore and D. A. Williams, Phys. Rev. B **59**, 7308 (1999).
- ⁷H. Hardtdegen, R. Meyer, H. Løken-Larsen, J. Appenzeller, Th. Schäpers, and H. Lüth, J. Cryst. Growth **116**, 521 (1992).
- ⁸H. Hardtdegen, R. Meyer, M. Hollfelder, Th. Schäpers, J. Appenzeller, H. Løken-Larsen, Th. Klocke, Ch. Dieker, B. Lengeler, and H. Lüth, J. Appl. Phys. **73**, 4489 (1993).
- ⁹H.-J. Hedbabny, Ph. D. thesis, Justus-Liebig-University Gießen, Germany, 1988.
- ¹⁰M. Gurvitch, J. P. Remeika, J. M. Rowell, J. Geerk, and W. P. Lowe, IEEE Trans. Magn. **21**, 509 (1985).
- ¹¹G. E. Blonder, M. Tinkham, and T. M. Klapwijk, Phys. Rev. B **25**, 4515 (1982).
- ¹²K. Neurohr, A. A. Golubov, Th. Klocke, J. Kaufmann, Th. Schäpers, J. Appenzeller, D. Uhlisch, A. V. Ustinov, M. Hollfelder, H. Lüth, and A. I. Braginski, Phys. Rev. B **54**, 17 018 (1996).
- ¹³R. Watts-Tobin, L. Kramer, and W. Pesch, J. Low Temp. Phys. **17**, 71 (1974).
- ¹⁴A. A. Golubov and M. Yu. Kupriyanov, J. Low Temp. Phys. **70**, 83 (1988).
- ¹⁵This Hall voltage contribution would lead to an offset of the differential resistance in Fig. 3 proportional to the magnetic field.
- ¹⁶The longitudinal resistance of the 2DEG in the investigated structure is for low magnetic fields much smaller than the contact resistance R_c and for high magnetic fields much smaller than the resistance $R_H = U_H/I_{ac}$ due to the Hall voltage.
- ¹⁷R. J. Haug, Semicond. Sci. Technol. **8**, 131 (1993).
- ¹⁸D. Uhlisch, M. Yu. Kupriyanov, A. A. Golubov, J. Appenzeller, Th. Klocke, K. Neurohr, A. V. Ustinov, and A. I. Braginski, Physica B **225**, 197 (1996).
- ¹⁹M. Büttiker, Phys. Rev. B **38**, 9375 (1988).
- ²⁰A. F. Andreev, Zh. Eksp. Teor. Fiz. **46**, 1823 (1964) [Sov. Phys. JETP **19**, 1228 (1964)].
- ²¹G. F. Giuliani and J. J. Quinn, Phys. Rev. B **26**, 4421 (1982).
- ²²Th. Schäpers, M. Krüger, J. Appenzeller, A. Förster, B. Lengeler, and H. Lüth, Appl. Phys. Lett. **66**, 3603 (1995).
- ²³D. Uhlisch, Ph.D. Thesis, Ber. Forschungszentrum Jülich Jül-3490, 1998.